

Received November 27, 2020; reviewed; accepted February 12, 2021

## Morphological changes of glass bead particles upon an abrasive blasting as characterized by settling and flotation experiments

Behzad Vaziri Hassas <sup>1</sup>, Onur Güven <sup>2</sup>, Esra Baştürkcü <sup>3</sup>, Mehmet S. Çelik <sup>3,4</sup>

<sup>1</sup> Department of Energy and Mineral Engineering, College of Earth and Mineral Sciences, Pennsylvania State University, University Park, PA 16802, US

<sup>2</sup> Adana Alparslan Türkeş Science and Technology University, Faculty of Engineering, Department of Mining Engineering, 01250, Sarıçam, Adana, Turkey

<sup>3</sup> Istanbul Technical University, Faculty of Mines, Department of Mineral Processing Engineering, 34469, Maslak, Istanbul, Turkey

<sup>4</sup> Harran University, Rectorate, Şanlıurfa, Turkey

Corresponding author: [oguvener@atu.edu.tr](mailto:oguvener@atu.edu.tr) (Onur Guven)

**Abstract:** The recent developments in mineral processing led researchers to look for alternative methods and propose new mechanisms for enhancing the efficiency of relatively costly processes (e.g., flotation, aggregation), where especially dealing with fine particles. Finer the particles, the higher the role of their surface on their behavior and properties. The importance of particle morphology becomes even clearer when particle-particle and particle-bubble interactions are considered. In this study, the effect of particle shape “roundness” on the surface wettability and flotation response was investigated upon producing fine particles with the “abrasion blasting” method. In order to provide a fundamental perspective, adsorption measurements were also carried out along with the flotation experiments under the same conditions. In addition to these, zeta potential measurements were also carried out with both spherical and blasted particles as a function of collector concentration. The results suggested that the roundness of particles decreased up to a certain nozzle pressure value, which was followed by higher adsorption degrees and consequently higher flotation recoveries. Additionally, settling rate tests were also performed with very fine material to show the effect of particle morphology on particle-particle interactions. The results showed that while lower settling rate values were obtained for spherical ones, higher values were obtained in the case of the ground and blasted samples in the presence of DI water. It was concluded from this study that the “Abrasive blasting method” could be an effective alternative for tuning the surface morphology of particles and their wettability, which in turn can affect the particle-particle interactions in the system.

**Keywords:** roundness, flotation, settling rate, energy barrier

### 1. Introduction

In mineral processing, size reduction, especially grinding, is the first step for producing particles of desired size and liberation before various enrichment methods. Although the size reduction to obtain the suitable size range for liberation and downstream processes is the main target in the grinding, its side effects on the particle surface, e.g., oxidation, roughness, shape factor, etc. should also be taken into consideration (Pourghahramani and Forsberg, 2005; Mahmoud, 2010). Due to different grinding mechanisms, each grinding method and type (wet or dry) have a specific effect on the surface roughness and the particle shape of the ground product. Therefore, the effect of different grinding conditions on particle morphology has been investigated by several researchers for various type of minerals such as barite (Ulusoy et al., 2003; Turk et al. 2018), talc (Yekeler et al., 2004), wollastonite (Little et al., 2015), glass bead (Rezai et al., 2010; Verelli et al., 2014; Hassas et al., 2016; Guven et al., 2016), quartz (Ulusoy

et al., 2004; Guven et al., 2015), alumina (Guven et al., 2016), and gold (Wotruba et al., 2015). Moreover, researchers have also related these variations of the particle morphology to the wettability through contact angle measurements on the mineral surfaces (Drelich and Marmur, 2017; Feng and Nguyen, 2017). In addition to minerals, researchers have also shown that low ash coke particles can be better floated when they are more angular (Rong et al., 2019). Although the role of mineral density and particle size is known to affect the flotation rate constant (Eskanolu et al., 2018a) recent studies on the contribution of shape factor on flotation recovery reported that the flotation kinetics and the rate constant of angular particles were higher than that of spherical ones (Yin et al., 2018). Consequently, the results from various studies indicate that during the grinding to achieve the required liberation of the valuables from gangue minerals, with appropriate conditions and parameters of the system, the shape of the mineral particles can be tailored to achieve better particle-particle and particle-bubble interactions which can be of enormous significance in flotation process (Koh et al., 2009; Albijanic et al., 2012; Guven et al., 2015; Eskanolu et al., 2019a). Investigations on possible alternative methods to control and alter the particle shape and morphology during the grinding can provide new insight and a different point of view to understand the importance and role of these effects in flotation. These studies also lead to a clear understanding of how to tune conditions with such surface modifications to achieve the best efficiency in enrichment (Guven et al. 2015; Guven et al., 2016; Hassas et al., 2016; Eskanolu et al., 2018; Xia et al., 2018).

Abrasive blasting of particles is a technique with wide applications in industry and commercially is used (as sandblasting) for cleaning or removal of layers from surfaces. The mechanism of this technique is to accelerate the particles, e.g., sand, using air pressure and spray them towards the surface with high speed where they collide and chip a layer off the surface. It should be noted that the particles during the blasting, also chip and break, which results in surface modification of these particles. Consequently, the blasting can be used for particle surface and morphology alteration by adjusting the operating parameters such as blasting distance, nozzle diameter, and pressure (Djurovic and Jean, 1999; Jianxin and Taichiu, 2000). To the best of the authors' knowledge, only a few works have been reported to this alternative method to modify the particle morphology and their subsequent flotation. Guven et al. (2015) showed that the blasting not only produces more angular quartz particles but also improves flotation recoveries. In another study from the same group, better flotation results were obtained for blasted talc mineral which was more angular than un-blasted talc particles (Guven et al., 2015). Considering its industrial applicability in mineral processing, a thorough study on this method would provide an opportunity of improving the hydrophobicity of particles and accordingly achieving higher flotation recoveries and settling rate (upon coagulation) with lesser chemical consumption.

In this study, the blasting method with various parameters was utilized to change the morphology and roundness of glass beads to investigate the effects of particle shape and morphology on their flotation recovery and settling rate in the presence of hexadecyl trimethyl ammonium bromide (HTAB). Additionally, classical DLVO theory was also employed to further the theoretical analysis of the particle-particle interactions upon surface modification.

## 2. Materials and methods

### 2.1. Materials

The glass bead particles used in this study were standard safety glass beads in the size range of 90×700 µm obtained from Potters Industries, USA. The chemical analysis of the sample performed by the X-ray fluorescence (XRF) technique is presented in Table 1.

The glass bead particles were first treated with an acidic solution (2.5 v/v % H<sub>2</sub>SO<sub>4</sub> (Sigma Aldrich, 95-98 % Purity)) followed by a basic solution (2.5 w/v % NaOH (Riedel de Haen, >97 % Purity) as suggested in previous work (Hassas et al., 2016). Finally, the samples were washed with distilled water (Ocean Reverse Osmosis System, Turkey) The pH of the bulk solution was controlled before and after

Table 1. Chemical content of the glass bead samples

Component	Si	Na	Ca	MgO	Al	Fe
Ratio (%)	61.3	13.1	14.8	3.8	6.0	1.0

the washing process to prevent any further contamination. The slurry was subsequently filtered and dried at 85 °C in an oven overnight. Before the experiments, the sample was screened through 150 and 106 µm sieves to obtain a 150×106 µm size fraction for the blasting, image analysis, adsorption, flotation, and settling rate tests. Hexadecyl trimethyl ammonium bromide (*HTAB*, 99.9%) from Merc Chemicals was used as a collector and distilled water (18 MΩ.cm) was produced in the laboratory using a single distilled water purification system (Ocean Reverse Osmosis System, Turkey).

## 2.2. Methods

### 2.2.1. Abrasive blasting

As discussed before, grinding is one of the widely used methods for not only size reduction but also changing the surface of the particles in mineral processing (Ulusoy et al., 2003). In this study, in addition to grinding for size reduction, the blasting method was used to modify the morphology of the glass beads while keeping the particle size constant. Details on the method and procedure are given elsewhere (Güven et al., 2015). The schematic presentation of the experimental setup is shown in Fig. 1.

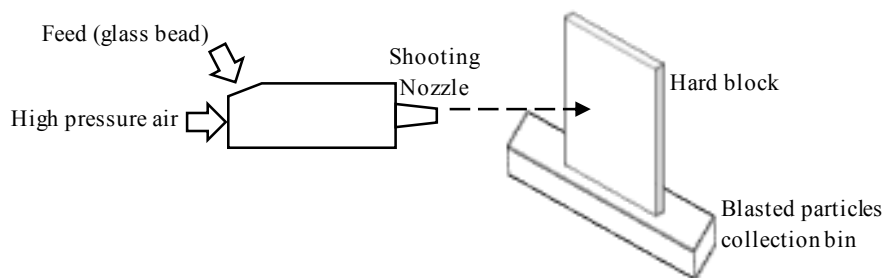


Fig. 1. Experimental setup for particle blasting

As depicted in Fig. 1, in order to modify the shape of particles, only nozzle pressure was controlled and changed in the range of 1 to 6 bar while the values of aforementioned parameters such as nozzle diameter (2 mm), feed rate (~60 g/min), and the distance between blasted surfaces and nozzle (19 cm) were taken constantly concerning the reported values in a recent study (Güven et al., 2015). Depending on the selected pressure, the velocity of the air coming out of the nozzle varies, so does the velocity of the particle. It should be noted that the trajectory of particles traveling towards the surface was perpendicular to the surface. As a result, the intensity of the collision between the particle (glass beads) and the hard plate is a function of the pressure difference which results in shape and roughness change.

### 2.2.2. Image analysis

The images of blasted glass beads were taken by binocular microscope (20X magnification) and processed using Leica Q-Win image analysis software. As reported in the literature, many parameters, such as elongation, aspect ratio, relative width, roundness, jaggedness, and chunkiness can be considered for evaluation of particle shape (Ulusoy et al., 2003; Yekeler et al., 2004; Rezai et al., 2010; Mahmoud, 2010; Eskinlou et al., 2019b). However, as extensively assessed in our previous studies, in research related to the flotation, roundness, and roughness can be considered as the most important parameters that influence the particle-particle and particle-bubble interactions (Güven et al., 2016; Hassas et al., 2016; Karakas and Hassas, 2016; Eskinlou et al., 2020). Therefore, in this study, the roundness of at least 300 particles was used for the characterization of the morphology and correlation of these effects with particle behavior in flotation and settling rates. The value of this parameter was calculated using Eq. 1 (Forsberg et al., 1990; Ulusoy et al., 2003).

$$R = \frac{4\pi A}{p^2} \quad (1)$$

where,  $A$  and  $p$  are the surface area and the perimeter of the particle, respectively. As the roundness ( $R$ ) decreases the shape of the particle deviates from the round shape (Hassas et al., 2016).

### 2.2.3. Zeta potential measurements

The surface charge of both spherical and blasted glass beads was investigated by zeta potential measurements. The change in surface charge (zeta potential) of glass beads was carried out as a function of HTAB concentration with a microprocessor equipped Zeta-Meter 3.0+ (USA). All the measurements were carried out under 75 V and K cell factor of  $0.71 \text{ cm}^{-1}$  (Sans et al., 2017) and  $10^{-3} \text{ mol/dm}^3$  KCl as background electrolyte. A sample of 0.1 g glass bead (below  $38 \mu\text{m}$ , with an average particle size of  $13 \mu\text{m}$ ) was added to  $100 \text{ cm}^3$  distilled water with the desired collector concentration, and the suspension was mixed for 10 min for sufficient adsorption. Particles from the supernatant of the suspension were taken for the zeta potential measurements. The average of at least ten measurements for each dispersion was recorded.

### 2.2.4. Adsorption measurements

Shimadzu UV-Vis mini-120 spectrophotometer was used for the adsorption analysis of HTAB on glass beads of various morphology at 195 nm wavelength. A calibration curve was obtained based on the UV absorption characteristics of HTAB of known concentrations as shown in Fig. 2. A calibration line with an  $R^2$  of 0.9964 was obtained.

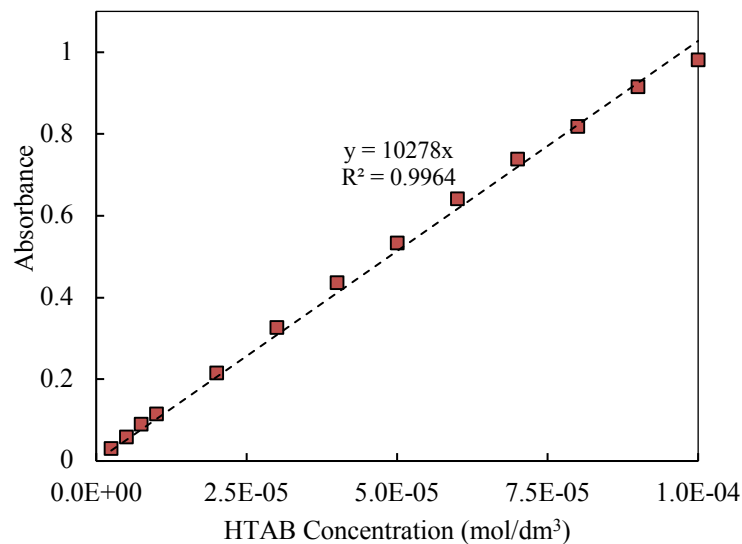


Fig. 2. HTAB adsorption calibration curve

For the adsorption experiments, 1 g of glass beads was placed in  $100 \text{ cm}^3$  of distilled water with predetermined HTAB concentration and stirred for 1 h at a constant room temperature of  $25 \text{ }^\circ\text{C}$ . Solids were then filtered, and the filtrate was tested with a UV spectrophotometer for the remaining HTAB concentration.

### 2.2.5. Micro-flotation experiments

Micro-flotation experiments were carried out using a  $155 \text{ cm}^3$  micro-flotation cell ( $30 \times 220 \text{ mm}$ ) with a fused silica frit (pore size of  $\sim 15 \mu\text{m}$ ), which was mounted on a magnetic stirrer as described in previous studies in more details (Güven et al., 2015). For each flotation experiment, 1 g of sample was conditioned in  $100 \text{ cm}^3$  distilled water with the desired collector concentration (1% wt.) for 10 min before the flotation. The solution was then transferred to the micro-flotation cell and floated for 1 min. The products were collected, dried, and weighed for further analyses. No frother was used in the flotation experiments. The pH of the glass bead suspension in distilled water was measured as 6.2 and did not show significant change during the experiments. High purity nitrogen gas was used for the aeration at a rate of  $50 \text{ cm}^3/\text{min}$ . Flotation recovery (eq. 2) in experiments was calculated based on the weight ratio of floated concentrate (C) to feed (F).

$$\text{Recovery}(\%) = \frac{C}{F} \times 100 \quad (2)$$

## 2.2.6. Settling experiments

Spherical, ground, and blasted glass beads of the same particle size were used in the settling experiments. Both the spherical and ground particles were used to demonstrate the extreme two sides of the morphological range. In each settling rate experiment, a 100 cm<sup>3</sup> measuring cylinder was filled with distilled water with the desired *HTAB* concentration containing 2 g glass bead making up 2 wt.% suspensions to provide free settling conditions as opposed to hindered settling which is prevalent in suspensions of above 15 wt.% (Taggart, 1945). The suspension was mixed three times by turning the graduated cylinder upside down to achieve a complete homogeneity without a pursuant flow regime inside the cylinder. This process was repeated before each run to standardize the conditions. The sedimentation mudline was recorded versus time as a function of *HTAB* concentration for the settling rate calculations. Each experiment was repeated thrice, and the average was taken as the final result. This procedure was repeated for both spherical and angular glass beads.

## 3. Results and discussion

### 3.1. Morphological characterization

The effect of blasting on the particle morphology was investigated in terms of variation in the roundness of glass beads that were produced upon blasting. For comparison purposes with the previous reports, the effect of blasting on various minerals and particles is depicted in Fig. 3. As seen from Fig. 3 that the roundness of the quartz particles of irregular shape did not change significantly by increasing nozzle pressure. However, at higher pressures, the roundness increased slightly, which can be ascribed to irregularities on the particle surface starting to chip off. Talc particles, on the other hand, showed a decrease in roundness in lower nozzle pressure, which increased again by increasing pressure (Güven et al., 2014, 2015c). This difference in the behavior of talc and quartz can be attributed to the minor difference in the density of the particles and the structural particle shape of the two minerals. The density of talc and quartz particles are 2.75 and 2.65 g/cm<sup>3</sup>, respectively. Particles of talc are flaky and with relatively lower density, hence, the effect of airflow on these particles can be more intense. As the airflow increases in the nozzle upon the increasing pressure, the drag force at higher pressure can affect the talc particles much easier compared to much heavier quartz particles. The drag force as a result of airflow can decrease the velocity and momentum of the talc particles and reduce the collision efficiency between the particles and surface.

A similar procedure was followed in this study, the variation on roundness values for glass beads (150×106 μm) showed that the roundness decreased from 0.956 to 0.836 up to 5 bar nozzle pressure. The pattern of change in roundness in glass beads of this study shows a variation from the previous research

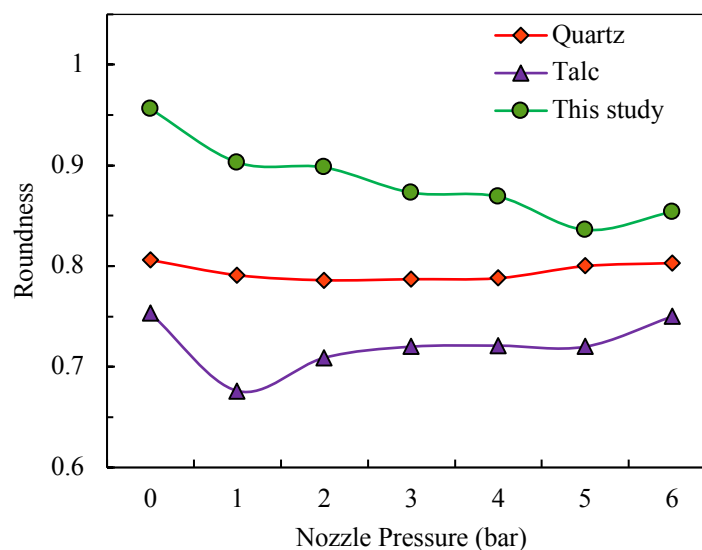


Fig. 3. Roundness values of different minerals: Quartz (Güven et al., 2015b), talc (Güven et al., 2015c), and glass beads (this study) as a function of nozzle pressure

(Güven et al., 2014). It should be noted that the quartz and talc particles in previous studies were ground to the target particle size, while in this study, the relatively bigger sample size was used to collect the target particle size using a sieve without grinding or size reduction in particles to preserve the original roundness of the glass beads. It is known that, during the grinding, the particle shape deviates from roundness due to the combination of different mechanisms such as abrasion, compression, which can result in sharp edges on the particles (Sirkeci et al., 2018). These edges and surface imperfections of the ground particles soften during the blasting, which can lead to an increase in roundness as the nozzle pressure increases. Consequently, the results shown in Fig. 3 indicated that the roundness of the quartz particles slightly increases at higher nozzle pressures. For other experiments in this study, the blasted glass bead particles were produced at 5 bar nozzle pressure.

### 3.2. Zeta potential measurements

The zeta potential measurements were carried out as a function of *HTAB* concentration, and a gradual increase in surface charge was observed upon increasing collector concentration up to  $10^{-4}$  mol/dm<sup>3</sup>. As seen from Fig. 4, while the zeta potential of untreated glass beads at pH 6 was measured as about -20 mV, an expected raise up to +30 mV was observed as a function of *HTAB* concentration. This trend can be well explained by the coverage of glass bead surfaces with the oppositely charged cationic reagent. Similar trends were also reported for other types of amine surfactants such as *DAH* (dodecyl amine hydrochloride) on glass surfaces. Asmatulu and Yoon (2012) reported that at  $10^{-4}$  mol/dm<sup>3</sup> *DAH* concentration, the surface charge of the glass increased from -60 mV to positive values while the contact angle also increased from 4° to 71° as an indication of increasing hydrophobicity and surface coverage by amine molecules. The increase in the zeta potential of the blasted glass beads was found to be greater at higher *HTAB* concentration compared to that of round glass beads. This can be attributed to the relatively higher specific surface area of blasted glass beads, which in turn results in higher *HTAB* coverage on the surface. A similar trend can be seen in adsorption experiments as well (Section 3.3).

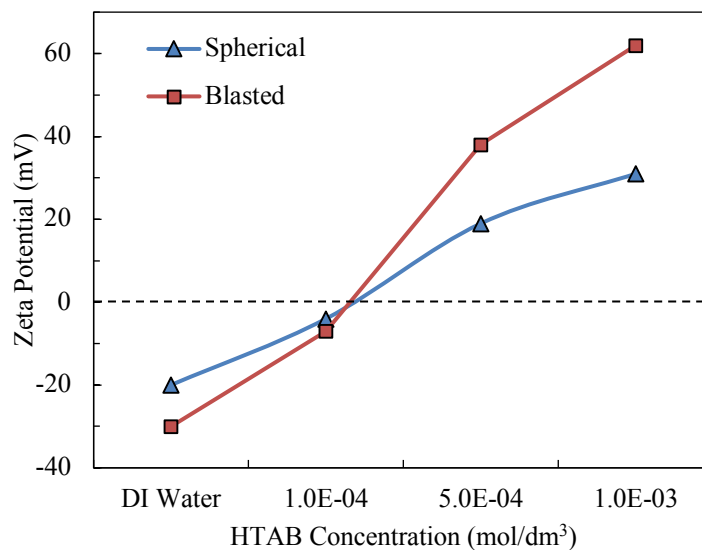


Fig. 4. Zeta potential of spherical and angular glass bead as a function of *HTAB* concentration at pH 6

### 3.3. Adsorption measurements

As well documented in the literature (Koh et al., 2009; Rezai et al., 2010), flotation recovery values are generally aligned with the reagent adsorption values, where higher adsorption also indicates higher flotation recoveries up to a critical concentration after which double layer formation on the surface renders it hydrophilic again. As discussed earlier, angularity in particles generally increases after the blasting process at different nozzle pressures (Fig. 3). It is noteworthy that the adsorption of *HTAB* molecules on the glass beads also follows the same pattern as roundness, however in reverse (Fig. 5). The adsorption of *HTAB* on the glass bead reaches a maximum at the nozzle pressure that produced the lowest roundness. This can be attributed to the specific surface area of the particles, as it is well-known

that the smallest ratio of surface area to the volume can be achieved at spherical particles. Hence, any deviation from sphericity will increase the specific surface area of the particles and in turn adsorption capacity, higher hydrophobicity, and a relatively higher probability of bubble-particle attachment in flotation.

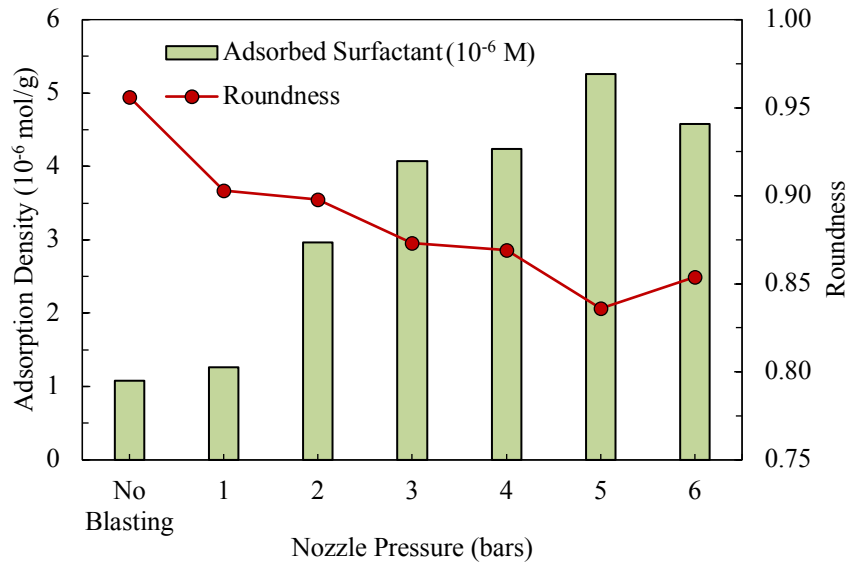


Fig. 5. Adsorption of surfactant on glass bead particles as a function of nozzle pressure

### 3.4. Micro-flotation experiments

Before the experiments with blasted materials, a series of micro-flotation tests were carried out as a function of *HTAB* concentration with spherical glass beads. The results indicated that the maximum recovery of  $\sim 70\%$  was obtained at  $10^{-4}$  mol/dm<sup>3</sup> *HTAB* concentration followed by a decrease at higher concentrations. This concentration coincides well with the surface charge results as the zeta potential of the glass beads turns positive at *HTAB* concentration above  $10^{-4}$  mol/dm<sup>3</sup> (Fig. 4). Bilayer adsorption and consequent decrease in hydrophobicity and flotation recovery have previously been reported in the literature (Somasundaran and Krishnakumar, 1997). Similar findings were also reported in other studies for quartz with dodecyl amine (Yoon and Yordan, 1990; Guven et al., 2015). Considering these results, two concentrations, i.e.,  $10^{-6}$  mol/dm<sup>3</sup> and  $10^{-5}$  mol/dm<sup>3</sup>, were selected for the maximum and minimum flotation recovery points to investigate the effect of blasting and shape factor.

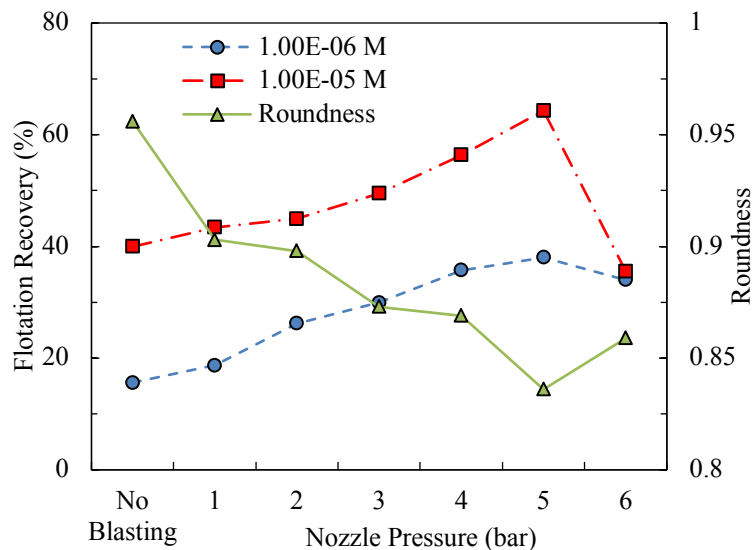


Fig. 6. The correlation between roundness and flotation recovery as a function of blasting pressure

As shown in Fig. 6, a steady increase in the flotation recovery at constant *HTAB* concentration was obtained for the particles blasted up to the 5 bars nozzle pressure for both concentrations. In other words, while the flotation recovery at  $10^{-6}$  mol/dm<sup>3</sup> *HTAB* concentration was 15% for spherical particles, it dramatically increased to 38% after the blasting. Likewise, for a constant  $10^{-5}$  mol/dm<sup>3</sup> *HTAB* concentration, the flotation recovery increased from 40% to over 64% by increasing the nozzle pressure in blasting. These findings suggest that the flotation characteristics of particles at a given collector concentration can be optimized by controlling their shape factor during the grinding or other pre-processing practices. As mentioned earlier, similar trends were also reported previously for products of various grinding methods and minerals (i.e., talc, calcite, barite, quartz, coal, and chromite) (Ulusoy et al., 2003; Yekeler et al., 2004; Koh et al., 2009; Rezai et al., 2010; Verelli et al., 2014; Little et al., 2015; Guven et al., 2016). Comparison of the flotation recovery values with particle roundness for various nozzle pressures illustrates that there is a well-established correlation between the two parameters (Figs. 3, 5, and 6). This indicates that the shape factor has a major role in the flotation response of the particles, which can outplay other weaker possible parameters in the process.

### 3.5. Settling experiments

For the settling experiments, in addition to distilled water, two different *HTAB* concentrations of  $10^{-5}$  mol/dm<sup>3</sup> and  $10^{-4}$  mol/dm<sup>3</sup> were selected to provide a comparison basis to the flotation recovery data. In these experiments, in addition to blasted and spherical particles, angular ones were also used to represent the effect of morphology on coagulation characteristics and therefore settling rate of the particles. The results of these tests are shown in Fig. 7. From the settling rate of the particles in distilled water, it is evident that the blasted and ground particles show a faster settling rate compared with that of spherical particles. This phenomenon has well been documented for the irregular-shape particles (e.g., ground particles) to exhibit lower resistance to the drag force in the motion in a fluid (Tran-Cong et al., 2004).

As shown in Fig. 7, it was found that the settling rate for all particles increases in presence of *HTAB*. It is well-known that the adsorption of *HTAB* on the particles renders the surface hydrophobic, which can result in further coagulation of the particles. Newly formed larger coagulated particles would become denser and heavier, which results in a faster settling rate of these particles. It is clear that, when the particles coagulate, the effective surface to volume ratio reduces, so does the effect of surface and morphology on the settling. This fact results in breaking the pattern of settling which was observed in distilled water. It is noteworthy that the settling rate at  $10^{-5}$  mol/dm<sup>3</sup> *HTAB* was higher than that in  $10^{-4}$  mol/dm<sup>3</sup> *HTAB* for all particles. This is in good agreement with other results reported in this study that the  $10^{-4}$  mol/dm<sup>3</sup> *HTAB* level is above the optimum concentration of collector molecules on the particle surfaces. Since the blasted and ground particles have a higher specific surface area, and higher adsorption capacity (Fig. 5) compared with the spherical particles, a significant amount of this excess *HTAB* concentration at  $10^{-4}$  mol/dm<sup>3</sup> *HTAB* can be consumed by these particles due to higher adsorption capacity. Consequently, the decrease in the settling rate in  $10^{-4}$  mol/dm<sup>3</sup> *HTAB* for the spherical particles is sharper than that for the blasted and ground particles, respectively.

### 3.6. Energy barrier analysis

As well known, in classical *DLVO* theory, the total *DLVO* energy component includes the sum of attractive van der Waals ( $V_{vdW}$ ) and repulsive electrostatic forces ( $V_{EDL}$ ) (Mao et al., 1999). However due to its short effective range, in most of the systems, the energy barrier height is dominated by only the influence of electrostatic forces while vdW forces remain negligible. In this context, the key point to pay attention is to the calculation of the surface potentials of particles that are the main variable parameter on the variation of energy barriers (Güven et al., 2015). The correlation of these values with their corresponding settling rates has not been studied in detail. Therefore, in this study, the extent of particle-particle interactions was evaluated to explain their coagulation mechanism as a function of collector concentration.

The van der Waals and electrical double layer forces were calculated according to a derivative of the classical *DLVO* model specifically developed for explaining the interactions between polystyrene and quartz surfaces (Suresh and Walz, 1996). The interactions were calculated via Eqs. 3 and 4.



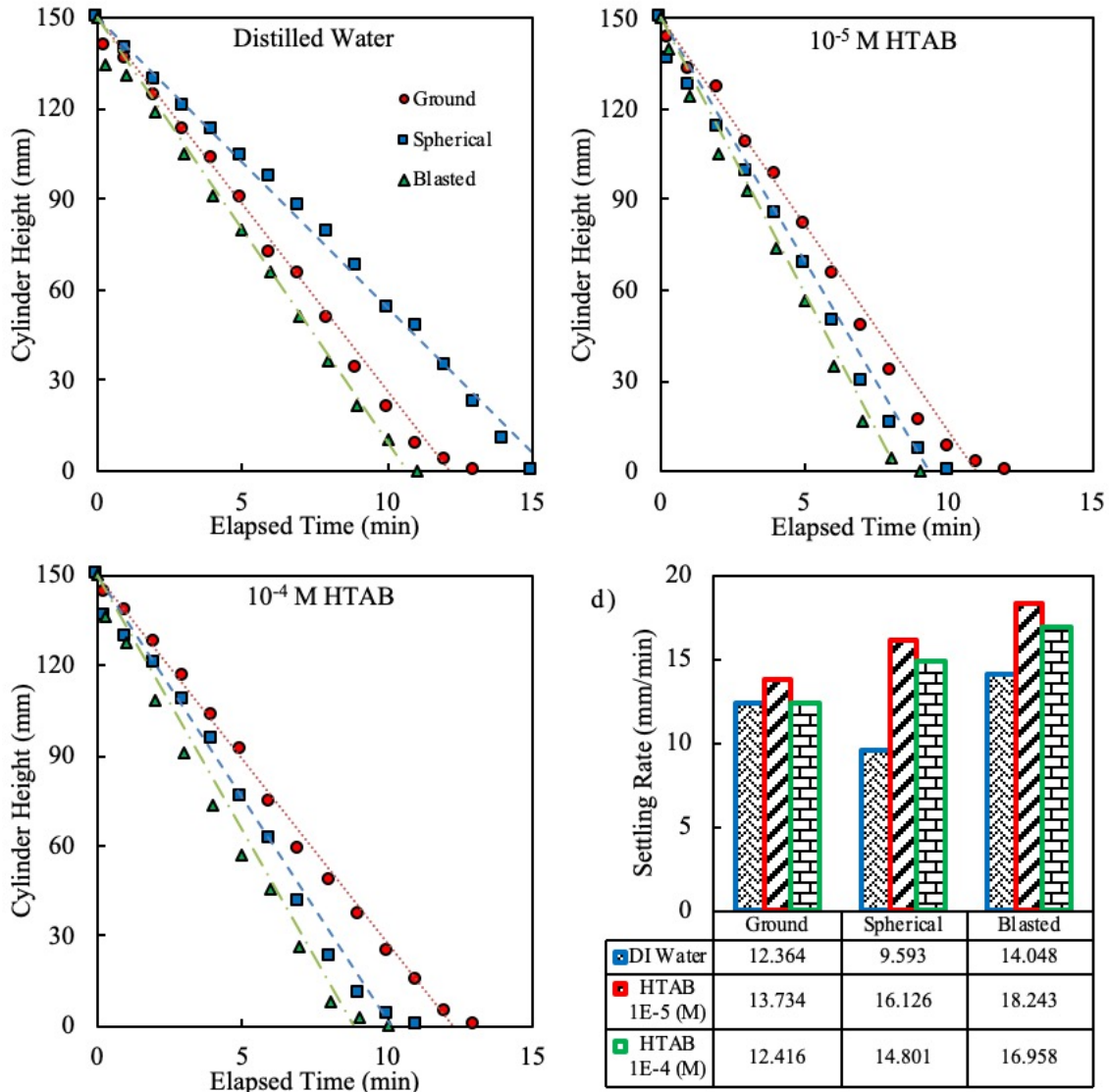


Fig. 7. The settling rate of spherical and angular glass beads as a function of HTAB concentration

$$V_{vdW} = 2\pi RA \left[ \frac{-2.45\lambda}{120\pi^2 h^2} + \frac{2.17\lambda^2}{720\pi^3 h^3} - \frac{0.59\lambda^3}{3360\pi^4 h^4} \right] \quad (3)$$

where  $A$  is the Hamaker constant,  $R$  is the radius of the spherical particle ( $\mu\text{m}$ ),  $\lambda$  is the characteristic wavelength,  $h$  is the separation distance (nm) as measured from the particle surface. Eq. 5 given below describes the electrical double layer forces:

$$E_{EDL-SS} = 16R(4\pi\epsilon\epsilon_0) \left( \frac{kT}{e} \right)^2 \tanh\left(\frac{e\psi_1}{4kT}\right) \tanh\left(\frac{e\psi_2}{4kT}\right) e^{-\kappa h} \quad (4)$$

where  $\psi_1$  and  $\psi_2$  are the surface potentials of the gas bubble and particle, respectively,  $k$  is the Boltzmann constant ( $1.38 \times 10^{-23} \text{ m}^2 \text{ kg s}^{-2} \text{ K}^{-1}$ ),  $e$  is the charge of a proton ( $1.602 \times 10^{-19} \text{ C}$ ),  $T$  is the temperature (298 K),  $\kappa^{-1}$  is the Debye length,  $\epsilon$  is the bulk dielectric constant (80),  $\epsilon_0$  is the permittivity of free space ( $8.85 \times 10^{-12} \text{ C}^2 \text{ J}^{-1} \text{ m}^{-1}$ ).

Energy barrier between particles as a function of distance for various HTAB concentrations is presented in Fig. 8. The results in Fig. 8 clearly showed that the energy barrier values exhibited a decrease with the increasing HTAB concentration. Thus, these results were somehow in line with their settling rate data presented in Fig. 7. If the minimum and maximum values were considered for each parameter ( $4.64 \times 10^{-16} \text{ kT}/\mu\text{m}$  at  $10^{-4} \text{ mol}/\text{dm}^3$  HTAB and  $7.40 \times 10^{-16} \text{ kT}/\mu\text{m}$  at  $10^{-6} \text{ mol}/\text{dm}^3$  HTAB), while the lower settling rate values (14.8 mm/min for  $10^{-4} \text{ mol}/\text{dm}^3$  HTAB) obtained at low energy barrier height value of  $4.64 \times 10^{-16} \text{ kT}/\mu\text{m}$ , higher values such as  $7.40 \times 10^{-16} \text{ kT}/\mu\text{m}$  were calculated for higher settling rate as 9.6 mm/min. These values were in line with those reported in recent literature

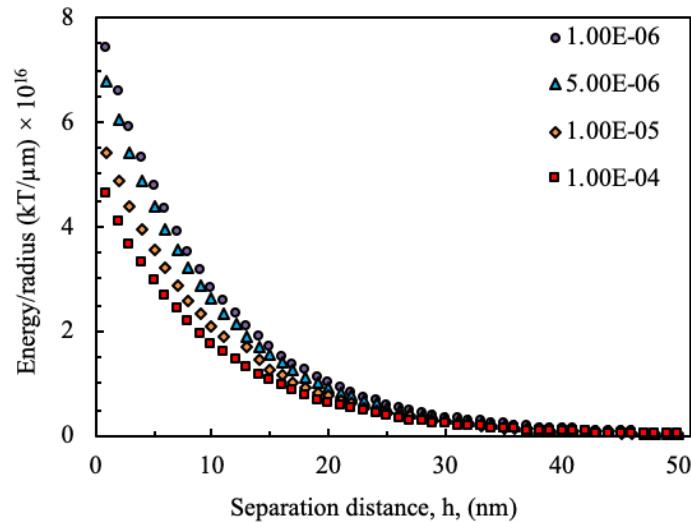


Fig. 8. Energy barrier between particles as a function of distance for various HTAB concentrations

where higher flotation kinetics were obtained at lower energy barrier heights. In other words, the flotation kinetics rate was 2.0 at the 40 kT/μm energy barrier whereas it was 0.9 at 100 kT/μm (Güven et al., 2015). Similar dependencies were also reported for the particle-particle interactions for coal-water slurries (Güven et al., 2016) where at higher reagent regimes the calculated energy barrier exhibited its minimum and due to increasing particle-particle interactions, the viscosity of suspensions became very high. Waltz et al. (1996) showed that with the increase of only the radius of asperities on surfaces from 0 to 40 nm, the secondary potential energy minimum decreased from 0.64 to 0.31 while the location of minimum was shifted from 44 to 70 nm indicating closer interactions between each surface. In another study by Bendersky (2013), it was found that decreasing the particle size from 5 μm to 0.5 μm resulted in lower energy barriers which were attributed to the attraction of smaller particles to the surfaces based on the decreasing zone of electrostatic influence. Considering that finding related to the effects of different parameters on interaction energy barriers, it can be suggested that better particle-particle interactions in the presence of higher collector concentrations could be obtained, and this would concurrently be followed by higher settling rates and energy barrier heights (Fig. 9).

As shown in Fig. 9, the settling rate increases at the concentrations where the energy barrier is low, which results in easier coagulation of the particles. On the other hand, the higher energy barrier prevents the coagulation of particles and consequently leads to better suspension and lower settling rates.

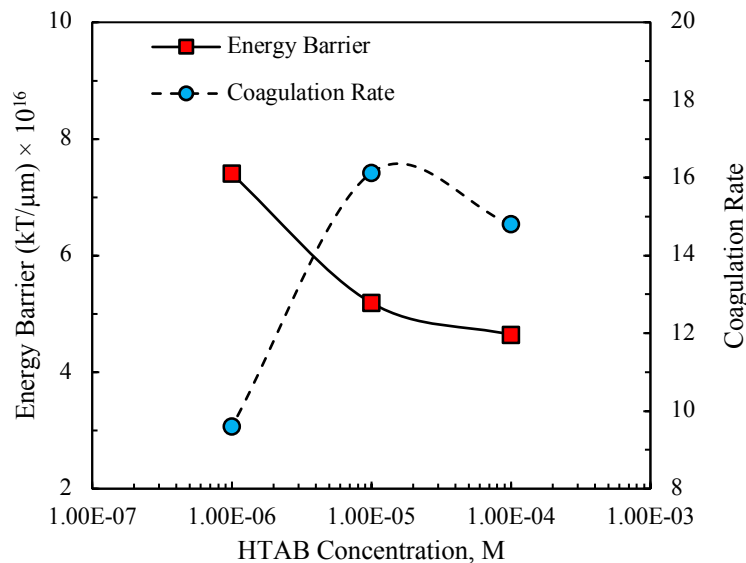


Fig. 9. Energy barrier calculation as a function of HTAB concentration

#### 4. Conclusions

In this study, the contribution of the abrasive blasting method on morphological features of glass bead particles on their flotation and settling characteristics was extensively investigated along with the zeta potential and adsorption tests. The results of these tests showed that while the roundness of spherical particles was measured as 0.956 before the blasting experiments, it gradually decreased to 0.854 upon applying 5 bars of blasting. Then, the flotation experiments were carried out with these blasted particles at  $10^{-5}$  and  $10^{-6}$  mol/dm<sup>3</sup> HTAB concentrations and yielded the flotation recoveries of 15.62 % and 39.97 % for un-blasted particles, and they increased up to 38.0 % and 64.3 % upon blasting at 5 bars. Accordingly, while the adsorption rate was measured as  $1.08 \times 10^{-6}$  mol/g for un-blasted particles, it increased to  $5.26 \times 10^{-6}$  mol/g for the particles blasted at 5 bars. This finding, in turn, showed that tuning the morphology of particles would also enhance the adsorption of collectors on their surfaces and concurrently their flotation characteristics. The settling characteristics of un-blasted and blasted particles also indicated that while the settling rate was found as 16.126 mm/min for un-blasted particles under  $10^{-5}$  mol/dm<sup>3</sup> HTAB concentration, it increased to 18.243 mm/min for blasted particles at 5 bars under the same conditions. Thus, the results of these series of tests also showed that the morphology not only changed the particle-bubble interactions but also particle-particle interactions which were then proved by theoretical energy barrier calculations. The results of these calculations also showed that while the energy barrier between two particles were  $7.40 \text{ kT}/\mu\text{m} \times 10^{16}$  at  $10^{-6}$  mol/dm<sup>3</sup> HTAB concentration, it gradually decreased to  $4.63 \text{ kT}/\mu\text{m} \times 10^{16}$  upon increasing the concentration to  $10^{-4}$  mol/dm<sup>3</sup> and were inversely proportional to their settling rate which points to better particle-particle interaction. In conclusion, the results obtained from this study showed that tuning the morphology of glass bead particles with abrasive blasting method enhanced both particle-particle and particle-bubble interaction which in turn resulted in higher flotation recoveries and settling rate values.

#### References

- ASMATULU, R. and YOON, R.H., 2012. *Effects of surface forces on dewatering of fine particles*. Separation Technologies for Minerals, Coal and Earth Resources, 95-102.
- BASTRZYK, A., POLOWCZYK, I., SADOWSKI, Z., SIKORA, A., 2011. *Relationship between properties of oil/water emulsion and agglomeration of carbonate minerals*. Sep. Purif. Technol. 77, 325-330.
- BENDERSKY, M., 2013. *Particle-collector interactions in nanoscale heterogeneous systems*, Open Access Dissertations, 724.
- DJUROVIC, B. and JEAN, E., 1999. *Coating removal from fiber composites and aluminium using starch media blasting*. Wear, 224, 22-37.
- DRELICH, J. W., AND MARMUR, A. 2014. *Physics and applications of superhydrophobic and superhydrophilic surfaces and coatings*. Surface Innovations, 2(4), 211-227.
- ESKANLOU, A., SHAHBAZI, B. and VAZIRI HASSAS, B., 2018a. *Estimation of flotation rate constant and collision efficiency using regression and artificial neural networks*. Separation Science and Technology, 53(2), 374-388.
- ESKANLOU, A., KHALESİ, M.R., ABDOLLAHY, M. and HEMMATI CHEGENI, M., 2018b. *Interactional effects of bubble size, particle size, and collector dosage on bubble loading in column flotation*. Journal of Mining and Environment, 9(1), 107-116.
- ESKANLOU, A., HEMMATI CHEGENI, M., KHALESİ, M.R., ABDOLLAHY, M. and HUANG, Q., 2019a. *Modeling the bubble loading based on force balance on the particles attached to the bubble*. Colloids and Surfaces A: Physicochemical and Engineering Aspects, 582, 123892.
- ESKANLOU, A., KHALESİ, M.R., MIRMOGADDAM, M., HEMMATI CHEGENI, M. and VAZIRI HASSAS, B., 2019b. *Investigation of trajectory and rise velocity of loaded and bare single bubbles in flotation process using video processing technique*. Separation Science and Technology, 54(11), 1795-1802.
- ESKANLOU, A., HUANG, Q., HEMMATI CHEGENI, M., KHALESİ, M.R. and ABDOLLAHY, M., 2020. *Determination of the mass transfer rate constant in a laboratory column flotation using the bubble active surface coefficient*. Minerals Engineering, 156, 106521.
- FENG, D. and NGUYEN, A.N., 2017. *Contact angle variation on single flotation spheres and its impact on the stability analysis of floating particle*. Colloids and Surfaces A: Physicochem Eng. Aspects, 442-447.
- FORSSBERG, E., ZHAI, H., 1985. *Shape and surface properties of particles liberated by autogenous grinding*. Scandinavian Journal of Metallurgy, 14, 25-32.

- GUVEN, O. and CELIK, M.S., 2016a. *Interplay of particle shape and surface roughness to reach maximum flotation efficiencies depending on collector concentration*. Mineral Processing and Extractive Metallurgy, 37,6, 412-417.
- GUVEN, O. KARAKAS, F., KODRAZI, N., CELIK, M.S. 2016b. *Dependence of morphology on anionic flotation of alumina*. International Journal of Mineral Processing, 156, 69-74.
- GUVEN, O., CELIK, M.S., and DRELICH, J., 2015a. *Flotation of methylated roughened glass particles and analysis of particle-bubble energy barrier*. Minerals Engineering, 79, 125-132.
- GUVEN, O., OZDEMIR, O., KARAAGACLIOGLU, I.E., and CELIK, M.S., 2015b. *Surface morphologies and floatability of sand-blasted quartz particles*. Minerals Engineering, 70, 1-7.
- GUVEN, O., KARAKAS, F., YASAR, G., CELIK, M.S., 2015c, *Morphological Characterization of blasted talc particles on talc flotation*. Proceedings of the World Congress on Mechanical, Chemical, and Material Engineering (MCM 2015) Barcelona, Spain –July 20-21, 331,1-7.
- GUVEN, O., OZDEMIR, O. I.E. KARAAGACLIOGLU, CELIK, M.S., 2014, *Contribution of roughness and shape factors on flotation of glass beads*, IMPC, Chile.
- HASSAS, B.V., CALISKAN, H., GUVEN, O., KARAKAS, F., CINAR, M., and CELIK, M.S., 2016. *Effect of roughness and shape factor on flotation characteristics of glass beads*. Colloids and Surfaces A: Physicochemical and Engineering Aspects, 492. 88-99.
- JIANXIN, D. and TAICHIU, L., 2000. *Techniques for improved surface integrity and reliability of machined ceramic composites*. Surface Engineering, 16, 411-414
- KARAKAS, F., VAZIRI HASSAS, B., 2016. *Effect of surface roughness on interaction of particles in flotation*. Physicochem. Probl. Miner. Process, 52, 18-34
- KOH, P.T.L., HAO, F.P, SMITH, L.K., CHAU, T.T., BRUCKARD, W.J., 2009. *The effect of particle shape and hydrophobicity in flotation*. International Journal of Mineral Processing, 93, 128-134.
- LITTLE, L., BECKER, M., WIESE, J., and MAINZA, A. N., 2015. *Auto-SEM particle shape characterization: Investigating fine grinding of UG2 ore*. Minerals Engineering, 82. 92-100.
- MAHMOUD, M.A., 2010. *Effect of comminution on particle shape and surface roughness and their relation to flotation process*. International Journal of Mineral Processing, 94, 180-191.
- POURGHAMRANI, P. and FORSSBERG, E., 2005. *Review of applied particle shape descriptors and produced particle shapes in grinding environments. Part I: Particle shape*, Miner. Process. Extr. Metall. Rev. 26, 145 -166.
- REZAI, B., RAHIMI, M., ASLANI, M.R., ESLAMIAN, A., and DEHGHANI, F., 2010. *Relationship between surface roughness of minerals and their flotation kinetics*. In: Proceedings of the XI International Mineral Processing and Technology Congress, 232-238.
- SIRKECI, A.A., GUL, A., BULUT, G., OZER, M., GUVEN, O., PEREK, K.T., 2018. *The effect of crushing type on the efficiency of flowing film separation*. Physicochemical Problems of Mineral Processing, 54, 2, 601-608.
- SOMASUNDARAN, P. and KRISHNAKUMAR, S., 1997. *Adsorption of surfactants and polymers at the solid-liquid interface*. Colloids and Surfaces A: Physicochemical and Engineering Aspects, 123-124,491-513.
- TRAN-CONG, S., GAY, M. and MICHAELIDES, E.E., 2004. *Drag Coefficients of irregularly shaped particles*, Powder Technology, 139 (1), 21-32.
- TURK, T., PEREK, K.T., KARAKAS, F., CELIK, M.S., 2018. *Effect of grinding time on particle shape in barite/SDS flotation system*. Proceedings of 16th International Mineral Processing Symposium (IMPS 2018), 378-383.
- ULUSOY, U., YEKELER, M., 2004. *Variation of critical surface tension for wetting of minerals with roughness determined by Surtronic 3+ instrument*. International Journal of Mineral Processing, 74, 61-69.
- VERRELLI, D.I., BRUCKARD, W.J., KOH, P.T.L., SCHWARZ, M.P., and FOLLINK, B., 2014. *Particle shape effects in flotation. Part 1: Microscale experimental observations*. Minerals Engineering, 58, 80-89.
- SURESH, L. and WALZ, J.Y., 1996. *Effect of surface roughness on the interaction energy between a colloidal sphere and a flat plate*. Journal of Colloid and Interface Science, 183, 199-213.
- XIA, W., 2017. *Role of particle shape in the floatability of mineral particle: An overview of recent advances*. Powder Technology, 317, 104-116.
- YEKELER, M., ULUSOY, U., HICYILMAZ, C., 2004. *Effect of particle shape and roughness of talc mineral ground by different mills on the wettability and floatability*. Powder Technology, 140 (1-2), 68-78.
- YIN, W., ZHU, Z., YANG, B., FU, Y., YAO, J., 2018. *Contribution of particle shape and roughness on the flotation behavior of low-ash coking coal*. Energy Sources Part A Recovery Utilization and Environmental Effects, 636-644.
- YOON, ROE-HOAN and YORDAN, JORGE L., 1990. *Induction time measurements for the quartz353 amine flotation system*. Journal of Colloid and Interface Science, 141, 374-382.